

5.4.1 Discussion of the Constraint Lines

Considering the design window on the diagram, basically four types of restriction lines which constrain the design space to a design window can be realized:

1. constraint of the minimum mean wind velocity of 5 m/s within the summer months.
2. the CG-constraint line, where the centre of gravity lays in a stable area, so that disturbing roll moments can be avoided.
3. the area constraint line, the constraint of maximum mean wind velocity, since above this velocity the available segment surface area is less than the necessary area of the solar arrays. Thus the segment surface area is not enough to install the solar arrays, in as much this area of solar cells is necessary to produce the required electrical energy during the regenerative mission.
4. the constraint of maximum payload.

In the following we will describe and discuss the constraint lines in detail:

1. Constraint of the minimum mean wind velocity: In this case it is the minimum mean velocity of 5 m/s which we meet in the summer months at the 48° longitudinal (see figure 5.1). This value is taken as a basis to constrain the design space. For a long endurance mission within the summer months a HAP should be able to overcome these mean wind speeds over the mission duration. Of course the propulsion system is able to bring about greater peak velocities as well, but for determination of the mean energy consumption on board this value of wind speed is used as basis and in according to this the energy system is layout. These parameters restrict the design space from bottom up and give the minimum size of the HAP and hence also the minimum size of all other on board system especially the size of propulsion system and energy system.

2. CG-constraint line: For the description of the CG-constraint line the design window of the four mission scenarios are presented and compared with each other in figure 5.18. There the CG-constraint lines are recognizable. This line occurs by connecting the CG constraint points on the curves. The constraint point indicates that only designs at the right side of the curve are valid designs, where the entire centre of gravity lie in the stable area of beyond $D/4$ (figure 5.19). Since the solar arrays are integrated at the upper surface of the segments and raise the centre of mass, the additional weights have to be integrated at the bottom of the segments in form of payload or system components, in order to shift the centre of gravity in the stable area so that disturbing roll moments can be avoided. Moreover the course of the CG constraint line is characteristic for this kind of solar array technology and corresponding energy storage device with its specific mass.

Hereby this issue is discussed in detail by comparing the 4 diagrams:

By comparing the constraint points of the two diagrams for 2.5km altitude with each other (figure 5.18), it is observable that each HAP length along the CG constraint line belongs to a specific wind velocity. E.g. for 8.8m/s we have a length of 80m and for 8m/s we have a length of 60m. Thus these value pairs are inextricably linked to each other so that they are valid for both diagrams with two different type of electrical storages.

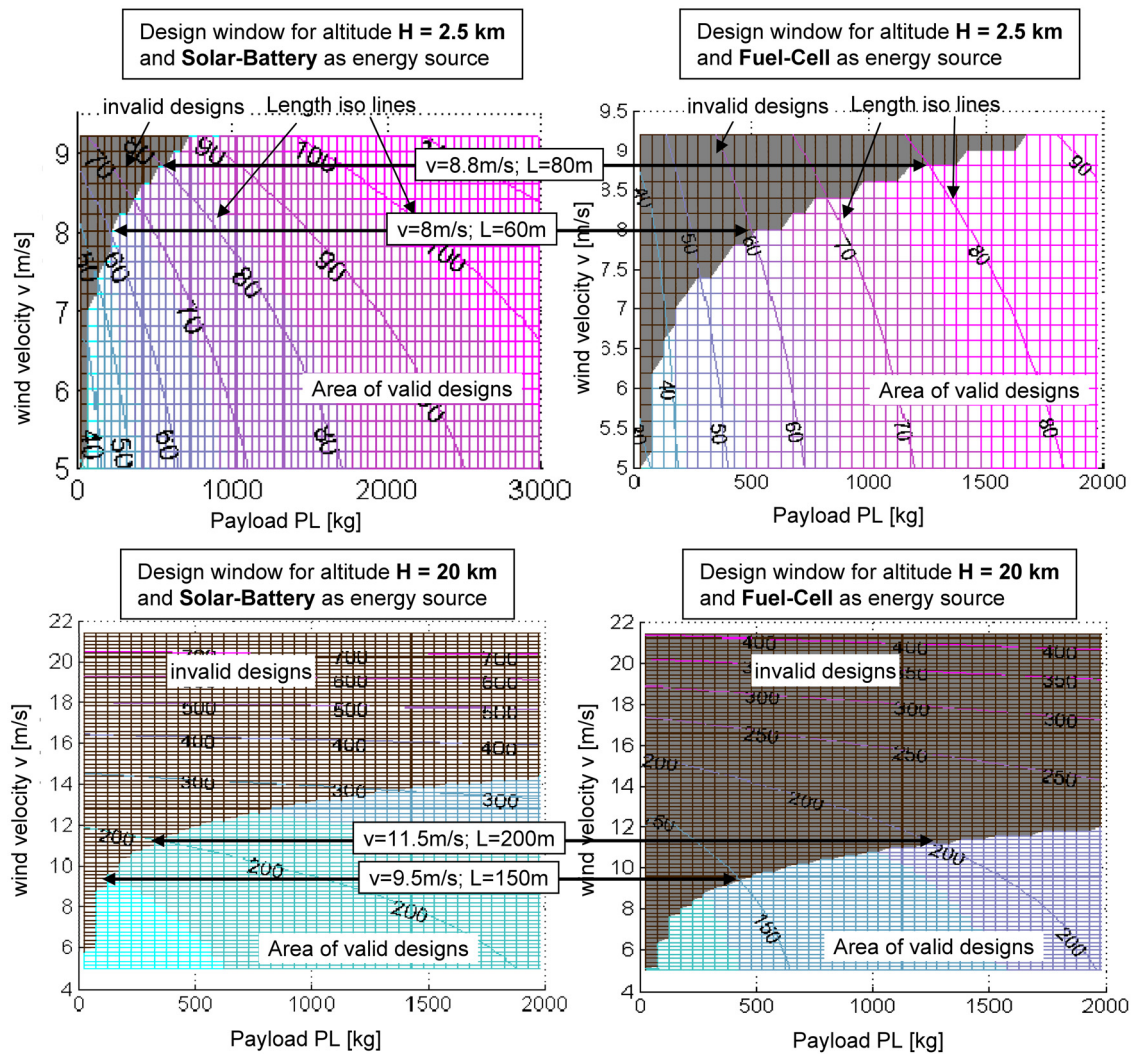


Figure 5.18: Comparison of design windows for description of the CG-constraint line for both energy storage concepts: batteries and hydro fuel cell; for flight in 2.5 km and 20km altitude and solar arrays with $1.5\text{kg}/\text{m}^2$ and 19% efficiency

The corresponding constraint length to each velocity is characteristic for this type of solar array technology with the specific mass of $1.5\text{kg}/\text{m}^2$ and 19% efficiency and can not fall below this limit. Here we compare designs of regenerative missions with same solar array type but two different types of energy storage concepts. The one is the battery system with $156\text{Wh}/\text{kg}$ and the other one is the hydro fuel cell with $1.866\text{kWh}/\text{kg}$, thus almost

12 times higher energy density than a battery. Since the solar arrays are integrated at the upper surface of the segments and the energy storage is integrated at the bottom of the segment, it has to be made sure that the overall centre of gravity is below $D/4$ (figure 5.19). This can only be ensured by adding further weights at the bottom of the segments thus it is only possible above a certain size of LTA HAP. If this is not the case disturbances of roll moments are produced which cause risk that the LTA HAP can turn upside down. That's why it is important to make sure that the designs lay at the right side of the CG-line. By connecting all marking constraint points with each other a CG constraint line occurs which restricts the design space from the left side of the design surface. Therefore the position of this line is dependent on the solar array technology. Since these solar arrays are used for both energy system concepts, it means that the centre of mass of the solar arrays is at the same position corresponding to the z-axis for both concepts. Thus almost same counter mass has to be installed at the bottom of the segments in order to shift the overall centre of mass into a stable position of below $D/4$. In the first case such a counter mass exists in form of batteries. Since the fuel cell contains 12 times less mass for same energy storage capacity, the remaining mass is compensated by other type of mass such as payload mass. Therefore the design surface of the fuelcell concept is slender and stretched to the right side in comparison to the battery system. As mentioned before there exist same dependency between velocity and HAP length for both concepts along the CG constraint line, thus according to that the power consumption is also the same for each HAP length. Also the total mass for each velocity and HAP length for both concepts is equal. But because of the 12 times lighter fuel cell system the mass of energy storage system is also 12 times lighter than that of a battery system and therefore according to the mass difference a greater payload mass is necessary for same wind velocity and HAP length to compensate this mass difference and therefore the design window area is stretched to the right side in area of high payload masses for same wind velocities. This means that performing a design with this kind of solar array technology would result into a length of LTA HAP with its corresponding wind velocity which is always equally independent from the type of used energy storage system, since decisive is the position of the centre of gravity (figure 5.19). Thus according to the diagram in figure 5.18 a design for LTA HAP with 9m/s and 500kg payload implies a length of 61m which is at the left side of the CG constraint line and therefore out of the design window. However a length of 93m is chosen which is a point laying direct on the CG constraint line by resulting in a LTA HAP design with 2.1 tone additional ballast. By this way a design with stable CG position is achieved for a reasonable mission.

The same applies for the altitude of 20kms: There exists a CG constraint line which starts at a length of about 90m for about 8m/s wind velocity. Below this length between 80m and 90m there exists no such kind of restriction and the CG lies in a stable area. The same course of the curve can be found for the solar fuel cell technology. To each wind velocity belongs a specific length of LTA HAP along the CG line. The course of the

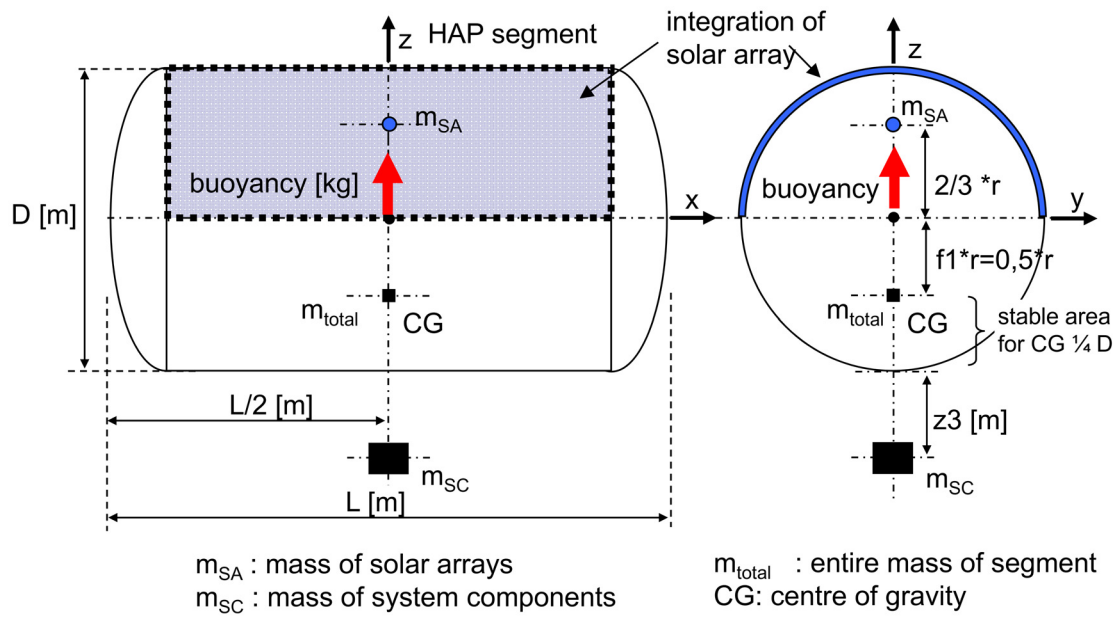


Figure 5.19: Crosssection of segment to illustrate the $D/4$ stable area of total mass m_{total} of segment; while m_{total} lying in this area occurs that the segment is atable against roll moments

graph is determined for this very solar array technology with its specific mass ($1.5kg/m^2$) and efficiency (19%) regardless of the used energy storage technology. But the shape of the entire design window is influenced by the used energy storage concept. For the solar battery system, the design window is broader and the CG line is steeper. Unlike the solar battery system, with hydro fuel cell system the design window is slender and prolonged to the right side of the diagram. Because the CG-line is flatter and therefore the intersection with the Iso lines of higher wind velocities occur only at larger payloads. As mentioned before this is the case because the hydro fuel cell storage system is almost 12 times lighter than the battery system, thus the remaining mass has to be compensated by the payload or by any other type of weights in order to shift the CG into the stable area of $\frac{1}{4}D$ (see also figure 3.17).

3. Area constraint line: Area constraint line is the line which restricts the design window from the upper side of the design space and is equivalent to the iso line of the maximum wind velocity. It means that the design can be performed only up to a specific velocity where the size of segment area is big enough to integrate the necessary area of the solar cells. Above this velocity the available segment area is smaller than the necessary solar array area and therefore not enough for this task. The value of this maximum velocity is determined by the solar array efficiency independent from its specific mass. Thus the upper side restriction line is determined only by the efficiency of the solar arrays. In case of 2.5km altitude and the solar array technology with 19% efficiency it is the mean

velocity of 9m/s which restricts the design window from the upper side. The curves in the diagram of figure 5.20 present the principle development of the areas of both, solar array and segment upper surface, dependent from the velocity. The increase of area of

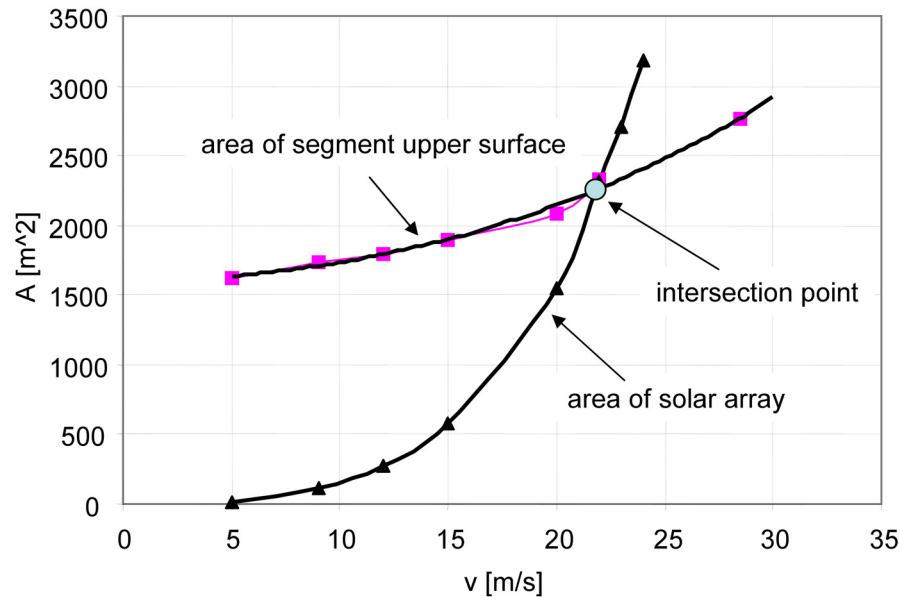


Figure 5.20: Principle development of areas of solar array and segment upper surface dependent from velocity, for flight in 20km altitude and specific payload, solar array efficiency, specific mass of solar array and electrical storage system.

solar array is steeper than that of the segment upper surface. Thus both curves have an intersection which is the maximum of the possible velocity for the design window. The same applies for the altitude of 20km altitude. In this case both curves have an intersection at a velocity of 22m/s for this efficiency of 19% unlike for 2.5km altitude with a maximum velocity of 9m/s. This is the case because of the much lower density in 20km altitude a much bigger volume of segments is necessary to carry the same payload as in 2.5km. Because of the bigger volume also the segment surface area is much bigger. Thus the increasement of segment upper surface area in 20km altitude is much steeper than that in 2.5km and therefore the intersection of both curves for 20km altitude has a higher value than that of 2.5km.

4. Constraint of maximum payload: The maximum payload depends on to what extent the envelope structure of the LTA HAP can be strained. Because the larger the payload the larger the total mass of LTA HAP and dependent on that is the structural strain of the envelope. Since in this work, the structural strength of the envelope is not superficially investigated, it is expected that the transferring of the forces into the envelope is arranged such advantageous that it is not overloaded and a mission operation can be performed without any problem up to a payload of 3 tone.

5.4.2 Comparison and Discussion of Design Space

variation of solar cell efficiency η_{SA} for duration $t \geq 24h$

Variation of parameters: η_{SA} solar cell efficiency, $m_{sp,SA}$ specific mass of solar array
 $m_{sp,FZ}$ specific mass of storage

Now we investigate the behavior of the design window by varying the parameters of solar array such as specific mass and efficiency. So far we have compared the results of two different altitudes that of 2.5km and 20km. For both we used solar cells with a specific mass of $1.5kg/m^2$ and an efficiency of 19% and two different types of electrical energy storage concepts, namely batteries with an energy density of 156Wh/kg and hydro fuel cells with 1.866Wh/kg. We investigated both short and long endurance missions and achieved thereby four different types of design spaces (figure 5.18). Especially the design spaces with regenerative energy systems were compared with each other in detail. It has been realized that the design space of each mission scenario is restricted in particular by four different types of constraint lines, which have been discussed in detail before. These are the constraint line of:

1. minimum mean wind velocity,
2. CG constraint line,
3. area constraint line with a maximum wind speed, and the
4. constraint of maximum payload.

According to that, all valid designs are lying in the design window which is spanned by these constraint lines. Disadvantageous is here the CG constraint line at the left side of the design window, which predetermined a minimum size of LTA HAP for increasing wind speeds and even for smaller payloads. Since for higher mean wind speeds of 9m/s the curve is simply cut up by the CG constraint line at a HAP length of 93m. Because only at this length the center of gravity is below the stable area of $\frac{1}{4}D$. In concrete terms, this means that for the whole payload interval between 3kg to 1400kg a minimum size of 93m has to be chosen for a mean wind speed of 9m/s, so that a stable flight can be performed at all. It is not possible to select a smaller HAP length for smaller payloads of e.g. 500kg, since all valid designs lay within the design window, thus at the right side of the CG constraint line. If one would however like to use a light weight and better energy storage such as hydro fuel cells which have about 12 times less mass for same capacity as batteries, this would not bring any advantages regarding the size of LTA HAP. Because the location of the CG constraint line is mainly influenced by the specific mass of the solar array. Thus for same type of solar arrays the minimum HAP length of 93m remains valid.

Regardless of which payload mass up to 1400kg or energy storage concept is selected, for this type of solar arrays the upper limits are predetermined as presented in the diagrams.

In the same manner, as the CG constraint line also the area constraint line is a disadvantageous limitation for the design of LTA HAP. Since the area constraint line is a boundary line valid for a specific mean wind velocity. It reveals that the size of the segment upper surface area is big enough to integrate the required solar arrays for only up to a wind speed of 9m/s in an altitude of 2.5 km. Above this wind speed the size of the solar array area exceeds the size of the segment upper surface area and can thus not be installed. Whereby, this limitation is predefined by the efficiency of solar arrays.

This means that the shape of the design window is mainly determined by these two parameters of the energy system, namely the specific mass and the efficiency. Because they have a significant impact on the size of entire LTA HAP design, therefore we will now investigate their influence on the shape of the design window.

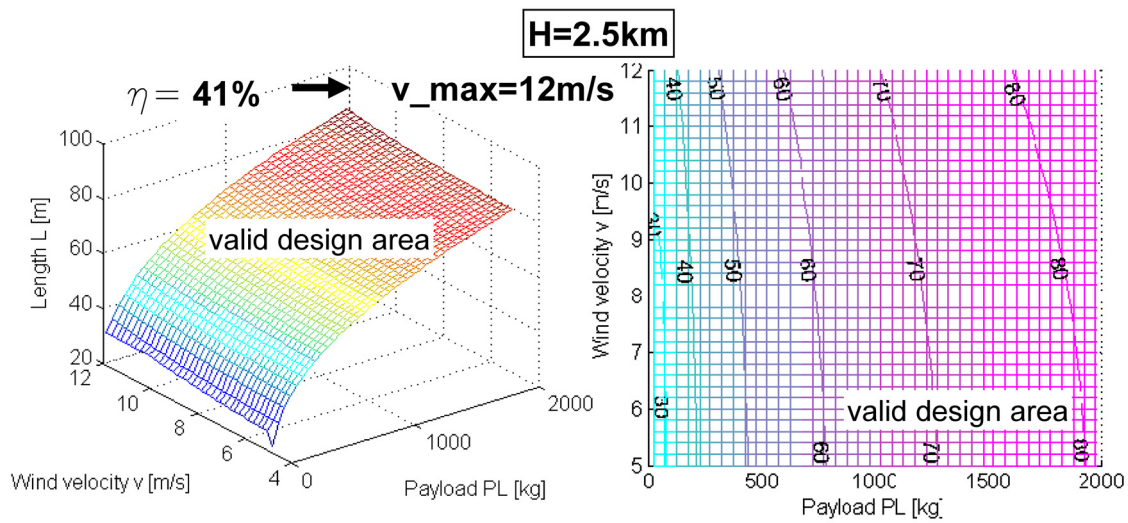
Following variation of the two parameters are undertaken:

Altitude: 2.5 km, fuel cell as regenerative energy storage system (figure 5.21):

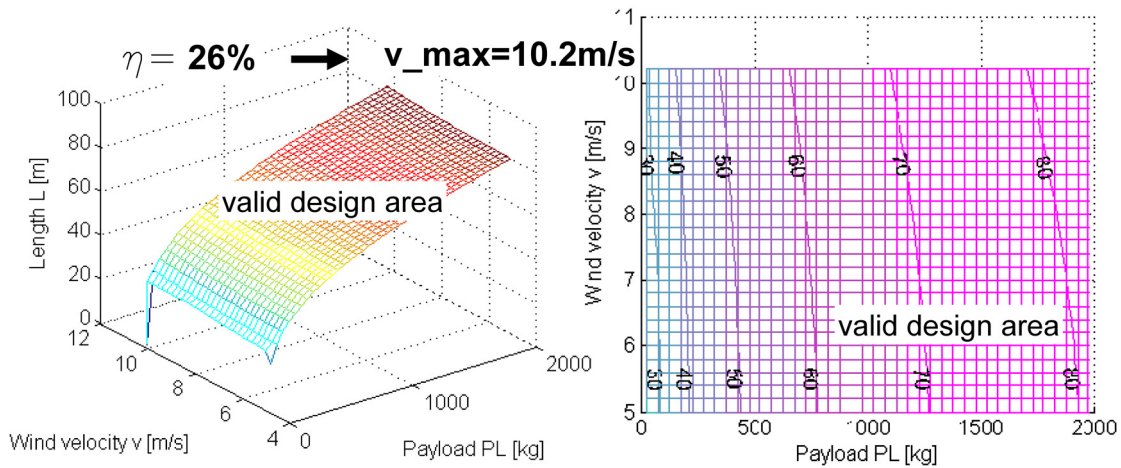
- a) Solar array specific mass: from $1.5\text{kg}/\text{m}^2$ to $0.25\text{kg}/\text{m}^2$
- b) Solar array efficiency: from 19% to 26%
- c) Solar array efficiency: from 19% to 41%

Altitude: 20 km, fuel cell as regenerative energy storage system (figure 5.22):

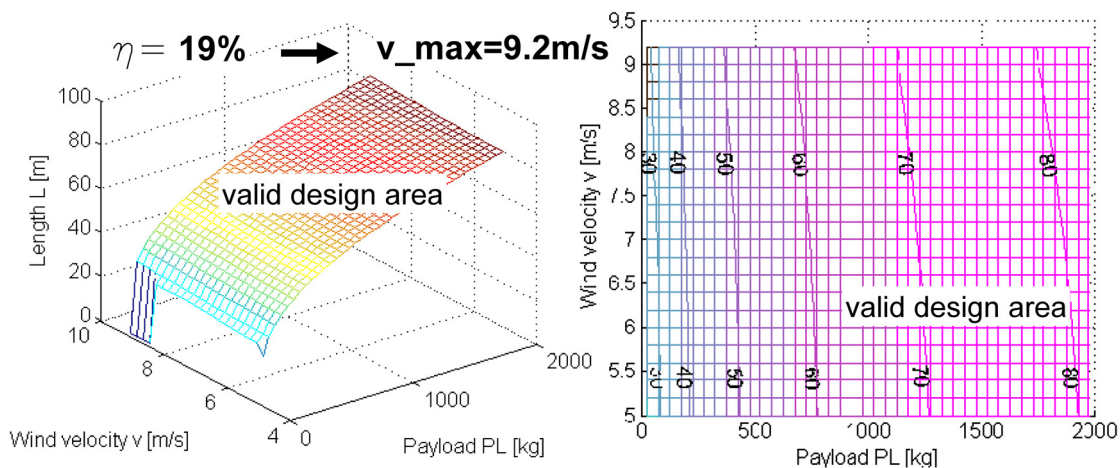
- d) Solar array specific mass: from $1.5\text{kg}/\text{m}^2$ to $0.25\text{kg}/\text{m}^2$ with η_{SA} 19%
- e) Solar array efficiency: from 19% to 26%
- f) Solar array efficiency: from 19% to 41%



c) H=2.5 km; Solar Array: 0,25 kg/m²; **Etha = 41%** ; Fuel Cell: 1,866 kWh/kg

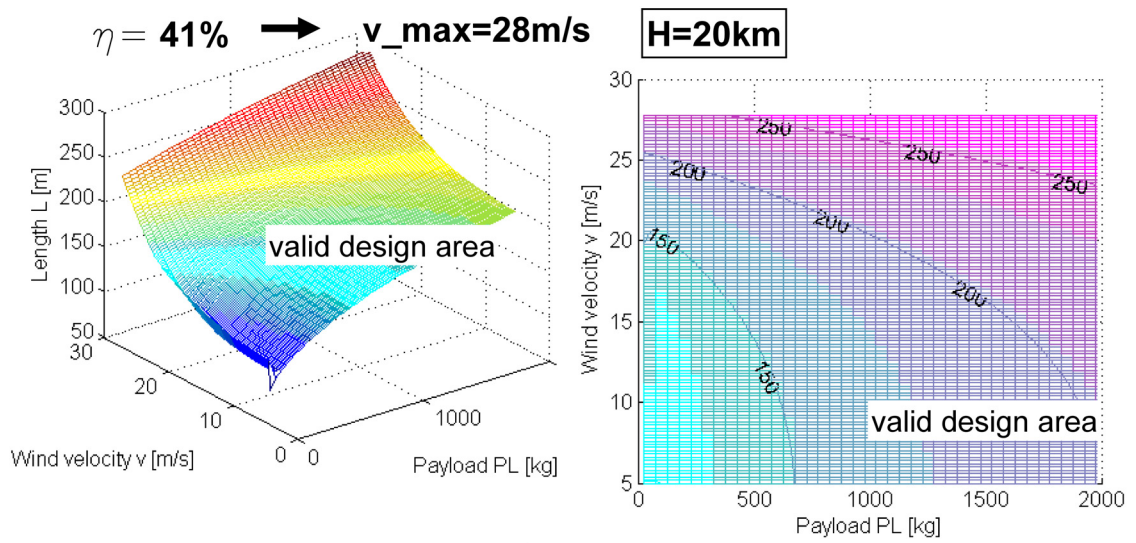


b) H=2.5 km; Solar Array: 0,25 kg/m²; **Etha = 26%** ; Fuel Cell: 1,866 kWh/kg

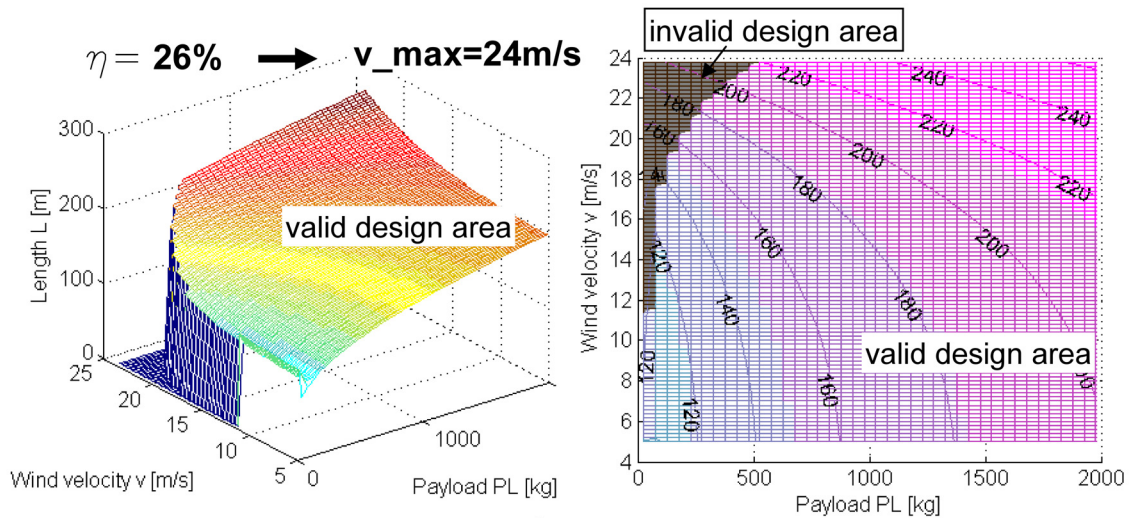


a) H=2.5 km; Solar Array: 0,25 kg/m²; **Etha = 19%** ; Fuel Cell: 1,866 kWh/kg

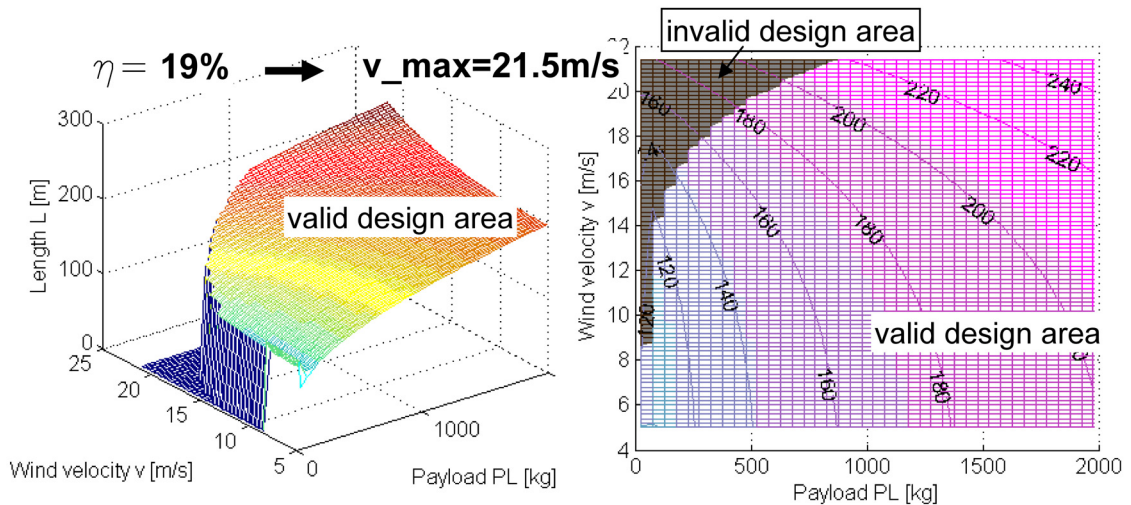
Figure 5.21: Comparison of design space for flight in 2.5 km altitude with a duration $t \geq 24h$ and variation of solar array efficiency; right diagram is top projection of the left diagram



c) H=20 km; Solar Array: 0,25 kg/m²; **Etha = 41%** ; Fuel Cell: 1,866 kWh/kg



b) H=20 km; Solar Array: 0,25 kg/m²; **Etha = 26%** ; Fuel Cell: 1,866 kWh/kg



a) H=20 km; Solar Array: 0,25 kg/m²; **Etha = 19%** ; Fuel Cell: 1,866 kWh/kg

Figure 5.22: Comparison of design space for flight in 20 km altitude with a duration $t \geq 24h$ and variation of solar array efficiency; right diagram is top projection of the left diagram

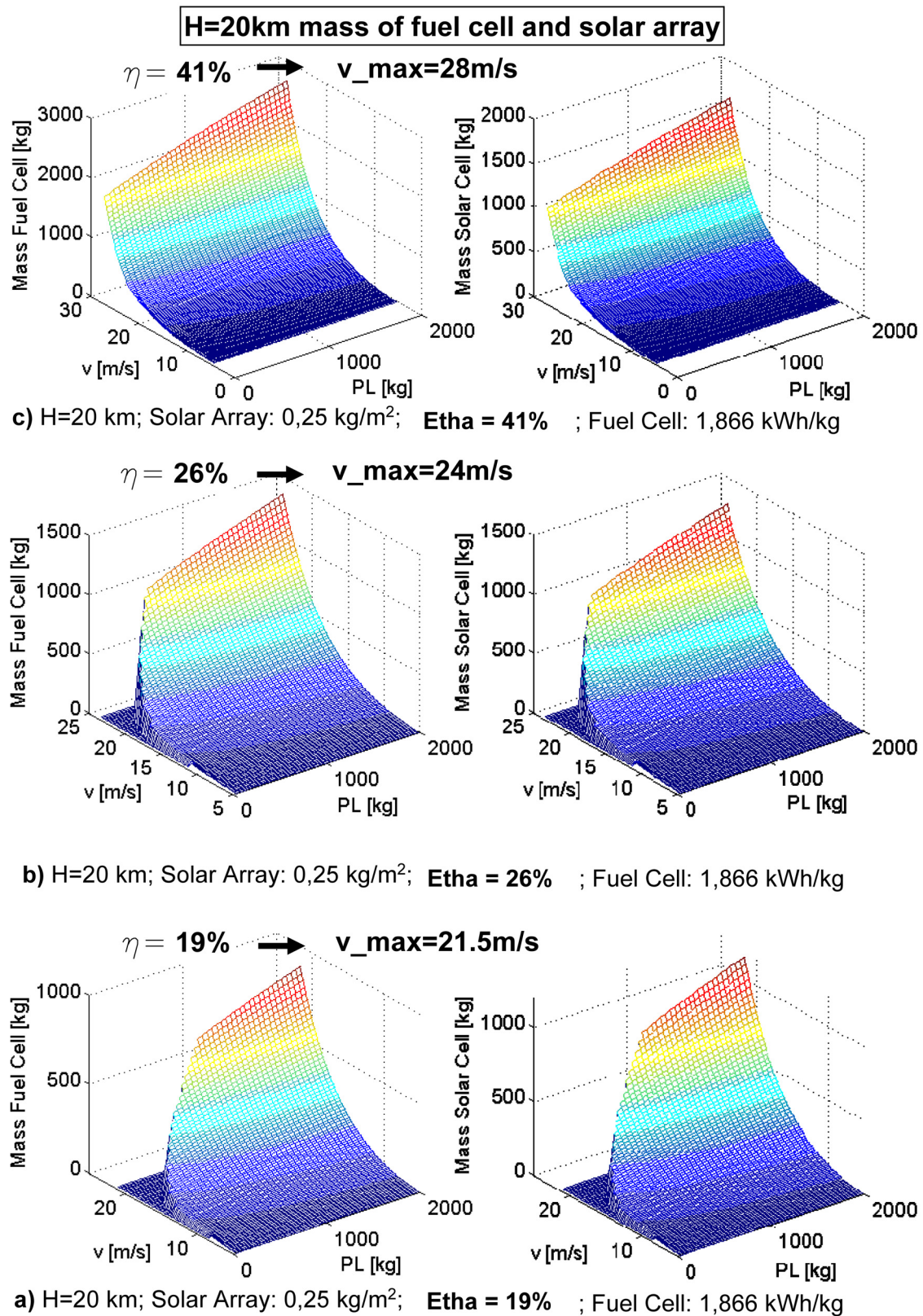


Figure 5.23: Comparison of diagrams of mass of solar arrays and fuelcell corresponding to the design surfaces presented in figure 5.22 for flight in 20 km altitude and variation of solar array efficiency

All 6 diagrams are presented in figure 5.21 and 5.22 and are described in the following: By changing the specific mass of the solar arrays for the 2.5km altitude, the CG constraint line shifts so far to the left side that it disappears. The design window moves also downwards so that for small payloads and velocities smaller sizes of LTA HAPs can be used. E.g. for a payload of 200kg and wind velocity of 9m/s even a HAP length of 43m can be used (figure 5.21 a)). In contrast to this, initial designs with heavier solar arrays enable this above a HAP length of 93m (figure 5.18). Moreover the design window is also slender. However, what does not change is the value of area constraint line for mean maximum velocity of 9m/s. Since this constraint line is only dependent on the efficiency of the solar array. Moreover this correlation is valid for both energy storage concepts, the batteries and solar-fuel cell system. In both cases of 2.5km altitude and 19% solar array efficiency the maximum mean velocity is 9m/s.

Now we change the solar array efficiency from 19% to 26% and the results are shown in figure 5.21 b).

The maximum mean velocity for the area constraint line increases from 9m/s to 10m/s. The design window is similar to variation a). By increasing the solar array efficiency to 41% we obtain 11.5m/s for the area constraint line (figure 5.21, diagram c). The design windows of all three variations have almost the same appearance. The curves on the design surface for the minimum wind velocity appears similar in all three diagrams. There is no CG constraint line and the area constraint lines have almost same curve shape, thus almost the same HAP lengths. This is because the growth of the maximum wind speed which is dependent from the solar array efficiency for the area constraint line is very flat.

The next variation is for 20 km altitude. There we have diagram a) in figure 5.22 for $0.25kg/m^2$ and 19% efficiency. The maximum wind velocity for the area constraint line is 22m/s. Unlike the 2.5km altitude here we can see that the CG constraint line still exists but it is moved very far to left, so that it appears at a velocity of about 15m/s and cuts the curve of 22m/s at a HAP length of about 210m. This point was with the heavier solar arrays of $1.5kg/m^2$ a length of more than 1200m and over 300,000kg payload. By increasing the efficiency the CG constraint line shifts to left and the value of maximum wind speed for area constraint line increases up to a value of 28.5m/s.

Figure 5.23 presents diagrams of mass of solar arrays and fuelcells corresponding to design surfaces presented in figure 5.22. As it is recognizable we were able to achieve a v_{max} of up to 28m/s but the corresponding diagram of solar array mass shows that a mass of up to 1,500kg is necessary. With 1,000kg we have a surface area of about $4,000m^2$ which is equal to an area of a football field. With 1,500kg we have a solar array area of more than 1.5 time of such a field.

Table 5.6 summarizes the results of variation of solar array efficiency. It is worth remembering that 19% efficiency of solar arrays is a value which is realistic, achievable

Altitude	2.5 km	20 km
η [%]	v_{max} [m/s]	v_{max} [m/s]
19	9	22
26	10	24.5
41	11.5	28.5

Table 5.6: Variation of solar array efficiency and corresponding maximum wind velocities of the area constraint line

and are available in the market. All other higher values are already laboratory confirmed but are not ready for series production and thus not available in such quantities in the market. Therefore all restrictions with 19% solar array efficiency are based on realistic conditions. All other calculations are based on assumptions that in the near future the solar array technology would be sufficiently mature and it would be available in sufficient commercial quantities.

Figure 5.24 presents the development of area of segment upper surface and solar arrays with the three different efficiencies of 19%, 26% and 41%. The diagram in figure 5.24 presents a design scenario at 20km altitude and a payload of 2000kg. Each curve of the

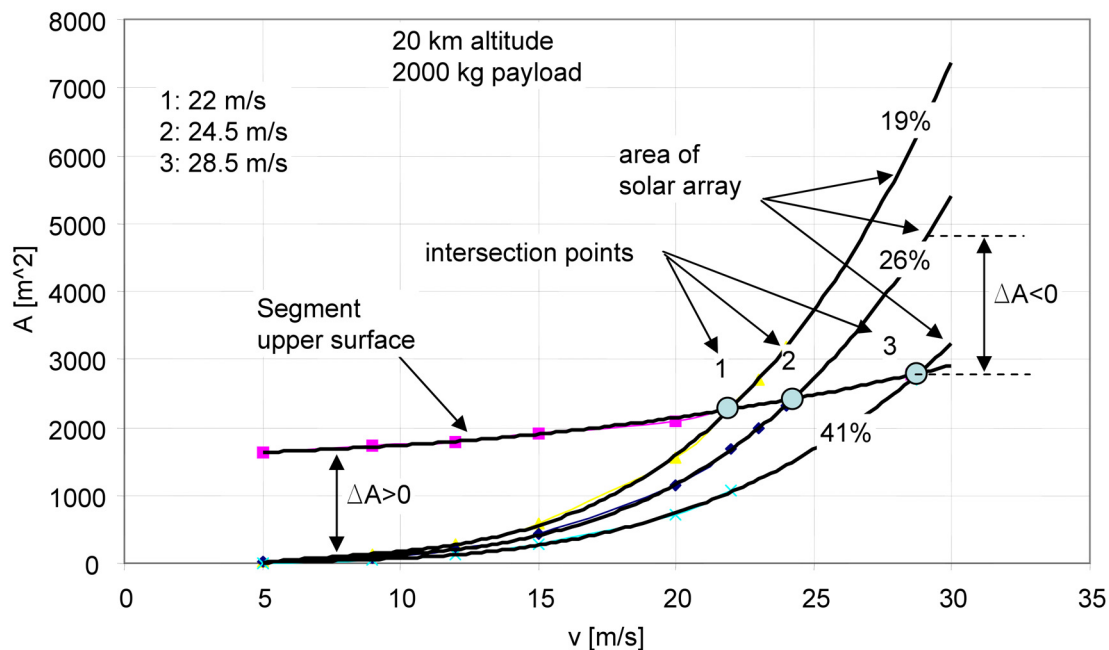


Figure 5.24: Variation of solar array efficiency and corresponding intersection points of segment surface area and solar array area for maximum wind velocities of the area constraint line

solar array area has an intersection with the curve of the segment surface. For a successful integration of the solar arrays on the segment surface it is necessary that the solar array area is smaller than that of the segment surface area. Thus the difference between both surfaces, ΔA , must always be greater than 0. With increasing velocity of wind and corresponding HAP length, the difference gets ever smaller until it is equal to zero at the point of intersection. At this point both surface areas are equal and it presents a limitation point of the design for the maximum velocity. Above this point the difference is smaller than zero and the segment surface area is not big enough to carry the solar arrays. Thus this point restricts the design window from the upper side of the design space. As mentioned before this graph is especially for the payload of 2000kg but the achieved result of intersection point is valid for all other payloads. With an efficiency of 19% the intersection point is lying at 22m/s. With increasing efficiency of the solar array the intersection point is shifted to the right side and we obtain 24.5m/s for 26% and 28.5m/s for 41%. Thus only with higher efficiencies of solar arrays the design barrier regarding area constraint line can be exceeded whereby HAP designs with higher wind speeds are achievable. Meanwhile the question of sufficient handling and integration of such football field sized solar array area remains still unsolved.

5.4.3 Comparison with Conventional Airship Design

Now we will adapt the geometry model of chainbody LTA-HAP to the geometry of a conventional airship such as HALE-D [78]. We will scale and morph this shape for analysis purpose. HALE-D is an UAV airship with a conventional geometrical form presented in figure 5.25. It is designed for flight in 20 km altitude with solar cells and batteries as energy source. We choose the state of the art in the market present technology to perform a design analysis to conventional airships. For this purpose 4 different design scenarios were calculated:

In design scenario 1 solar arrays with 19% efficiency and batteries with 156 Wh/kg are used (figure 5.26). With this technology a maximum velocity of 13m/s is achieved, but for a payload mass of 2000kg. For this design point a solar cell area of more than $1,000m^2$ (projection area) is required which has a mass of about 2500kg and the corresponding mass of batteries is 4,000kg.

In design scenario 2 we use thin film solar arrays which have usually an efficiency of about 7%. The calculation results are presented in figure 5.27. There we achieve a maximum velocity of up to 13.5m/s with a solar array area of up to $3,000m^2$ (projection area) which is $4,500m^2$ integration area. Which has a mass of about 2000kg. The required amount of batteries is about 4000kg.

In design scenario 3 we reduce the aerodynamic drag coefficient from $C_w=0.08$ to $C_w=0.05$

and were able to increase the v_{\max} up to a value of 16m/s. In design scenario 4 (figure 5.29) we increase the solar array specific mass to a hypothetical value of $0.25\text{kg}/\text{m}^2$ by $\eta = 19\%$. Furthermore fuelcells were used instead of conventional batteries with a value of 1,866Wh/kg. This is a 11 times lighter electrical storage technology as the conventional LiIo batteries. Thus we achieve a v_{\max} of up to 22m/s with a corresponding solar array area of more than 2000m^2 .

All these calculations are done for the summer months. For the winter months we have only a mean solar radiation of $200\text{W}/\text{m}^2$ in 20 km altitude for only 6 h during day time. Which means that 2.5 times less solar radiation is available for half time during the summer month. Thus for the winter months 5 times more solar array area of summer months is necessary to produce enough electrical energy to design an airship with same v_{\max} . This is with the state of the art technology of solar arrays not possible. Because if we need 3000m^2 solar array area during the summer months then we need 15000m^2 during the winter months. This an area of about 4 football fields and the upper surface of an airship did not provide such a surface. Furthermore the integration and handling of solar arrays with such quantities present problems of its own.

HALE-D Performance Parameters		HALE-D Characteristics	
Station-keeping Altitude	60,000 ft	Hull Volume	500,000 ft ³
Payload Weight	50 lbs	Length / Diameter	240 ft / 70 ft
Payload Power	500 watts	Propulsion Motors	2 kW Electric
Endurance	> 15 days	Energy Storage	40 kWh Li-ion Battery
Recoverable	Yes	Solar Array	15 kW thin-film
Reusable	Yes	Cruise Speed	20 ktas @ 60 kft

Copyright ©2008 Lockheed Martin Corporation
All Rights Reserved.
PIRA #AKN200807001
HAA_0106.qxd

MS2

Defense and Surveillance Systems
1210 Massillon Road
Akron, Ohio, 44315-0001 USA
www.lockheedmartin.com/ms2/product_contacts

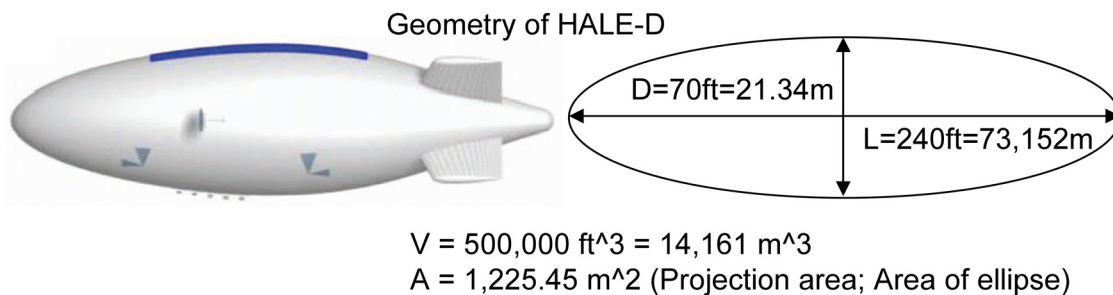


Figure 5.25: Shape of conventional airship HALE-D [78] which is scaled and morphed for further investigation

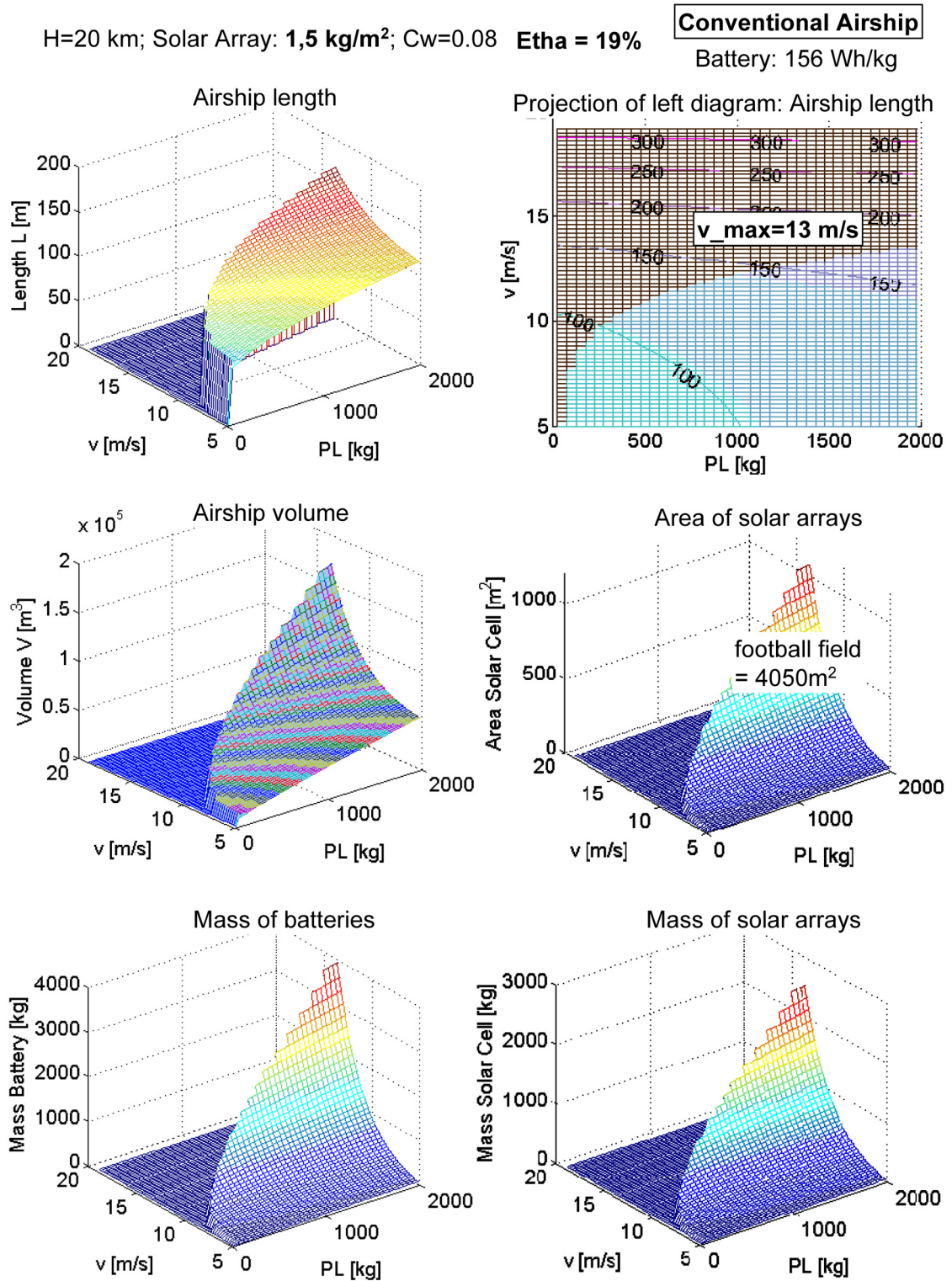


Figure 5.26: Conventional airship configuration 1: H=20km; duration $T \geq 24h$; solar array material: 1,5kg/m²; Cw=0.08; $\eta = 19\%$; energy density of battery: 156Wh/kg

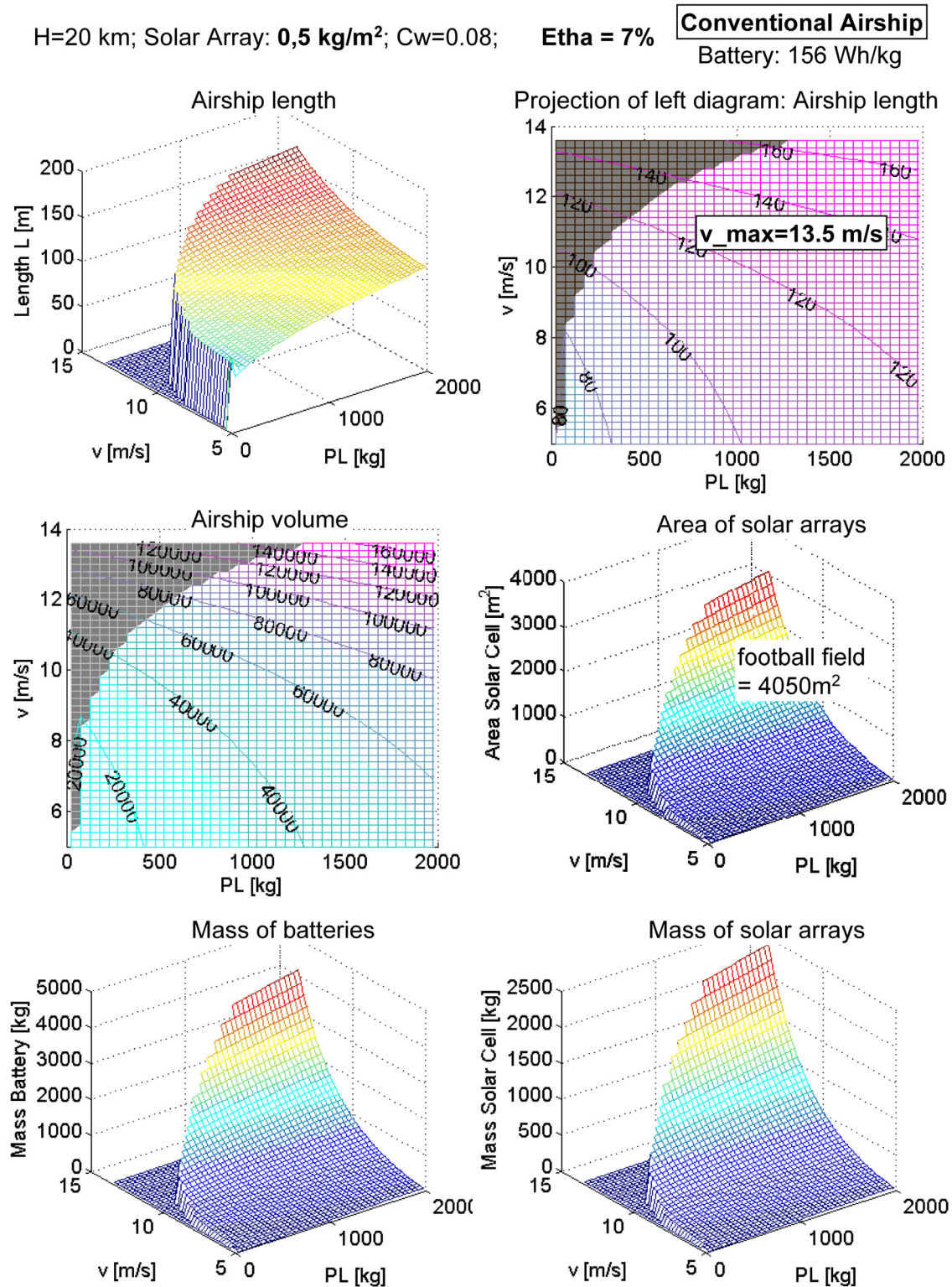


Figure 5.27: Conventional airship configuration 2: H=20km; duration $T \geq 24h$; solar array material: $0,5kg/m^2$; $Cw=0.08$; $\eta = 7\%$; energy density of battery: $156Wh/kg$

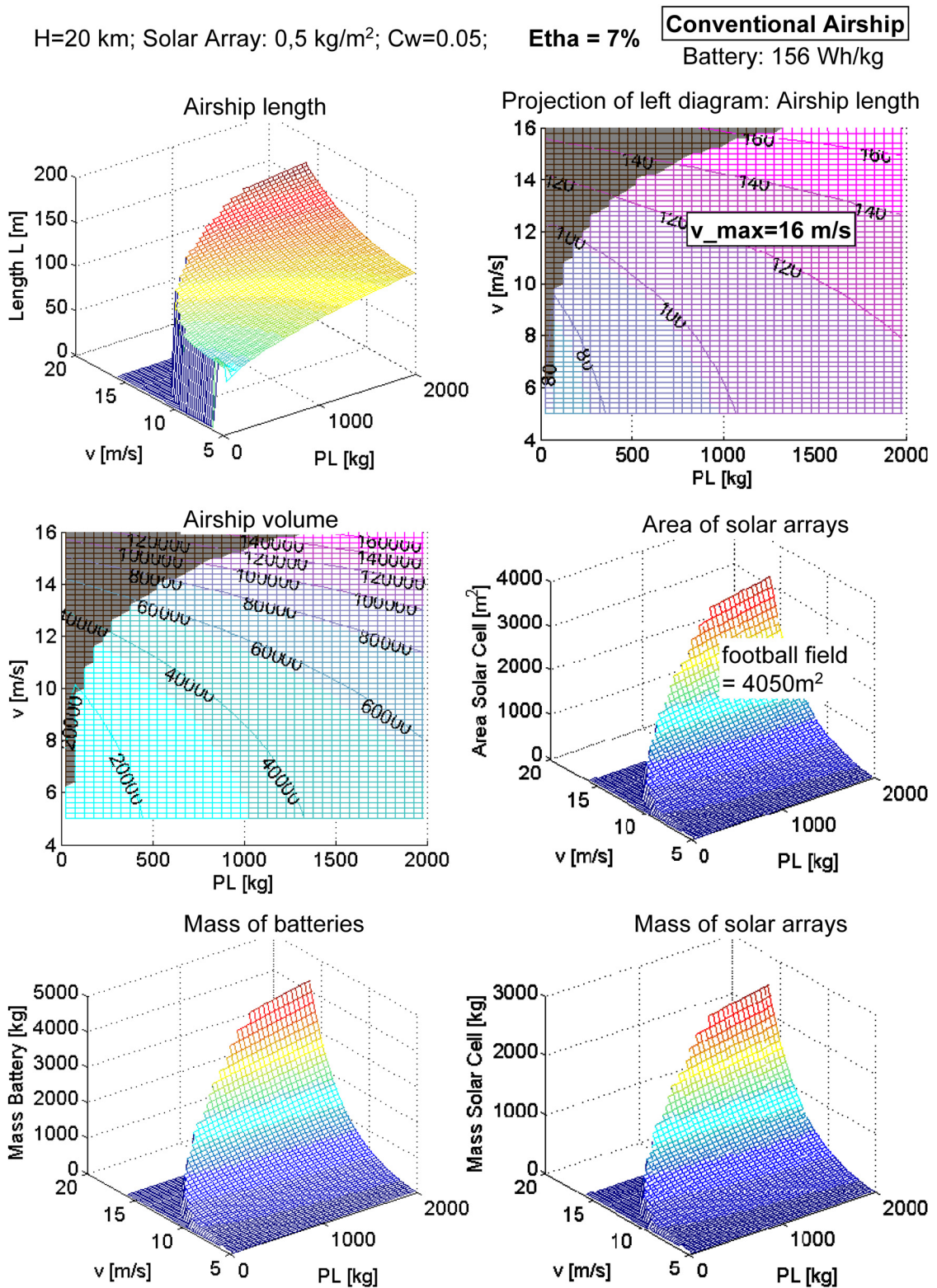


Figure 5.28: Conventional airship configuration 3: H=20km; duration $T \geq 24h$; solar array material: 0,5kg/m²; Cw=0.05; $\eta = 7\%$; energy density of battery: 156Wh/kg

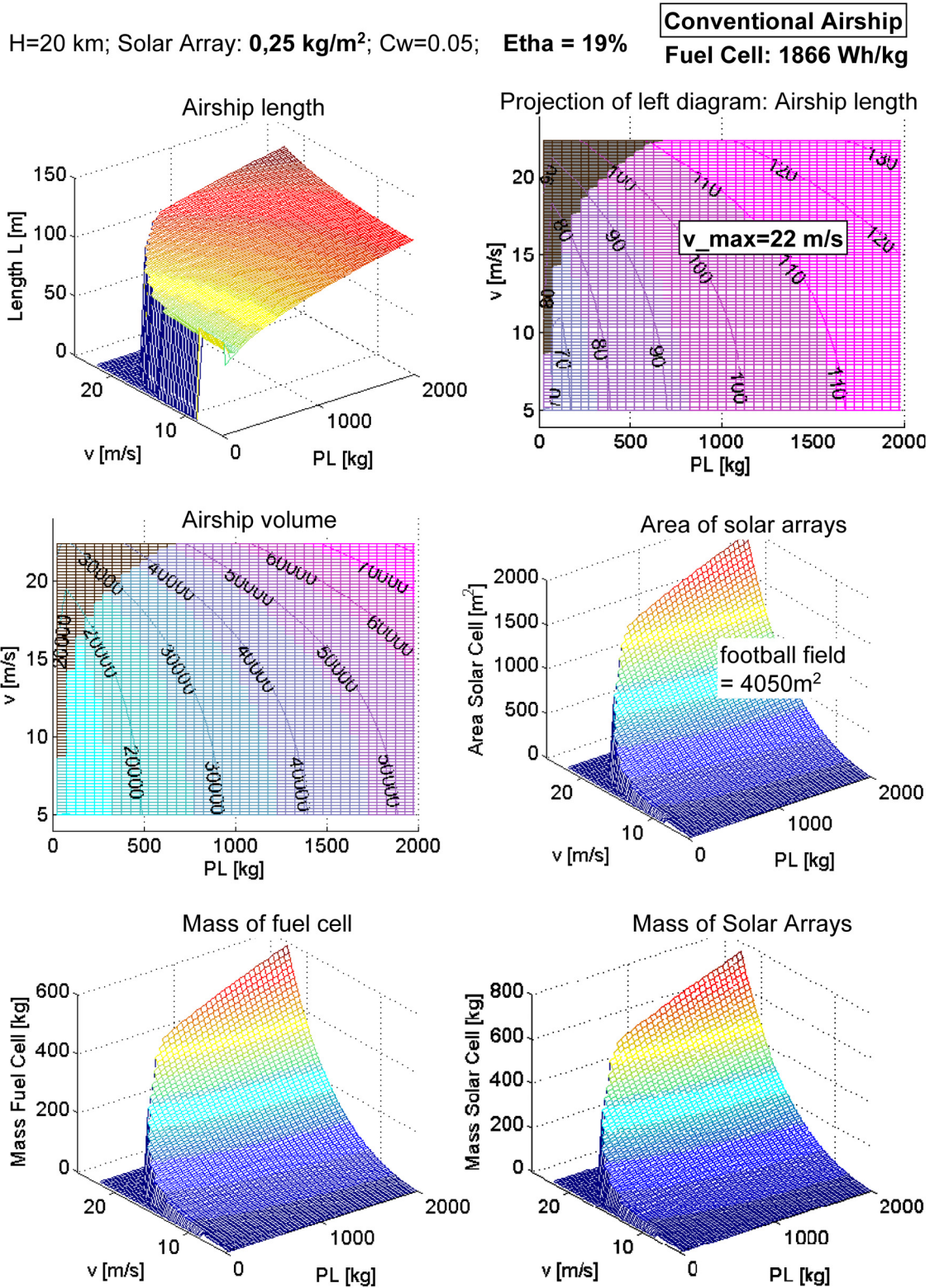


Figure 5.29: Conventional airship configuration 4: H=20km; duration $T \geq 24h$; solar array material: $0,25kg/m^2$; $Cw=0.05$; $\eta = 19\%$; energy density of battery: $1866Wh/kg$

5.4.4 Summary of the Results

With the method of rule based graph grammars an object oriented design analysis is performed to the mission of multi chain LTA HAP.

Two different flight altitudes, 2.5km and 20km were investigated within 5 different mission scenarios. For short duration missions LiIo batteries were used as energy source. Whereby for long endurance missions solar arrays were used in combination with energy storage for the night phases. As storage for electrical energy LiIo batteries(156W/kg) as well as hydro fuel cell system (1,866W/kg) were used. As a result we achieved design windows for the specific missions. For further investigations the four long endurance missions with regenerative energy systems were compared with each other. The comparison show that the design window within the design space is essentially restricted by 4 types of constraint lines:

1. minimum mean wind velocity,
2. CG constraint line,
3. area constraint line with a maximum wind speed, and the
4. constraint of maximum payload.

It is well clear for constraint line 1 and 4, that a minimum mean velocity has to be maintained and in regard to the payload there is maximum load capacity relating structural strength of the envelope. Therefore a specific strength analysis is not performed within this work, but it is assumed that a payload up to 2000kg could be carried by the hull structure without any strength problems. The method of graph grammars provides the opportunity to enhance the entire design model and integrate a structural strength analysis capability so that for each design point such an analysis can be performed and dealt as a constraint for the rule based approach.

Constraint lines 2 and 3 are investigated in detail, since they have a significant influence on the shape of the design window. The CG-constraint line is dependent on the specific mass and efficiency of the solar arrays and restricts the design space from the left side. The area constraint line is only dependent from the efficiency of the solar arrays and restricts the design space from the upper side. The design spaces are considered as contour maps in L-PL-diagrams (L=HAP length; PL=payload). For higher specific masses ($1.5\text{kg}/\text{m}^2$) and low efficiencies (19%) of the solar arrays one is forced to use large HAP size for even smaller payloads. Therefore it is a desirable goal to shift the CG-line as far as possible to the left side, so that small HAP sizes for smaller payloads can be used.

Since the solar array efficiency influences the location of the area constraint line, it presents a natural limit of maximum mean wind velocity for a long endurance mission

e.g. with 19% efficiency we have a limitation of 9m/s for 2.5km altitude and 22m/s for 20km altitude.

By improving the specific mass of the solar arrays from $1.5\text{kg}/\text{m}^2$ to $0.25\text{kg}/\text{m}^2$, it was possible to shift the CG constraint line so far to the left side so that smaller size of LTA HAPs could be used for smaller payloads, e.g. for $v_{max} = 22\text{m}/\text{s}$ the size could be reduced from a theoretical value of 1200m to a realistic value of 210m. Furthermore by improving the efficiency from 19% to 41% (hypothetical value) the limit of maximum velocity could be increased from 22m/s to 28.5m/s.

However by comparing the results following statements could be derived:

- In our northern latitude of 48.83° a station keeping mission is possible in 20km altitude by using state of the art solar cell technology ($1.5\text{kg}/\text{m}^2$ and 19% efficiency) and batteries as electrical storage (156Wh/kg). But such a mission is not possible in winter months, since five times more solar array area is required and the required speed of 39m/s can not be achieved.
- The specific mass and the efficiency of the solar arrays are the dominating parameters which primarily influence the shape of the design window within the design space. These are the parameters amongst others which have to be developed most likely, so that long endurance missions with more reasonable size of chainbody LTA HAPs and sufficient values of maximum mean velocities are possible. So that long endurance high altitude station keeping missions are possible during the whole year.

6 Conclusion

In this work a graph grammar based design language has been applied as an approach for multi disciplinary object oriented design analysis of lighter than air (LTA) high altitude platforms (HAPs).

The main contributions of this work are:

1. a systematic investigation to the innovative concept of multi disciplinary chainbody LTA HAP and design analysis for long endurance deployment in 20km altitudes,
2. development of an object oriented graph grammar based design language as a platform for systematic exploration and analysis of design space of LTA HAPs within a reasonable timeframe,
3. analysis of five different type of mission scenarios in order to identify the constraint lines delimiting design surfaces within the design space,
4. identification of design limitation parameters and their coupling to the design delimiting constraint lines for purpose of strategy development in order to conceive novel design solutions,
5. investigation of three different type of propulsion systems and their operational capability for long endurance deployment of LTA HAP in 20km altitudes.

The multi disciplinary object oriented design analysis is performed as following:

An object oriented design model is developed based on the method of graph grammars. For this purpose the objects, so called vocabulary, are defined which contain all kind of information such as geometry, physics, mathematical equations etc. for each discipline. The couplings between the objects are identified and defined as the rules of the grammar. Following disciplines are considered during the modelling process: envelope structure, aerostatic and aerodynamic, operational environment, energy storage and power supply system, propulsion system as well as system integration and power network. The design model is applied to calculate 5 mission scenarios in order to explore the design space. A mission is characterized by the used energy system such as (a) batteries, (b) a combination of solar arrays and batteries and (c) solar arrays and fuel-cells. The design analysis leads

to identification of boundaries that delimit the design surfaces within the design space, the so called constraint lines such as, (1) constraint line of minimum mean wind velocity, (2) CG-constraint line (3) area constraint line for the specific maximum wind speed, and the (4) constraint of maximum payload. Decisive are the constraint line (2) and (3), because they are defined by the parameters of used solar cells technology: the specific mass and the solar array efficiency. The CG-constraint line is influenced by both parameters. But the area constraint line is explicitly influenced by the solar array efficiency.

The results of the design analysis can be summarized as following:

With the developed design language chain body LTA HAPs were investigated in regard to their propulsion system based on various energy storage technologies. It has been found out that the use of state of the art propulsion system technology enables a long endurance deployment only within limited time windows of summer months. This is due to the fact that the solar arrays are installed at the upper side of the segment surfaces of multi chain LTA HAP. Thus designs for higher wind velocities demands accordingly larger solar array surfaces. But only a certain amount of solar arrays can be installed on the upper surface of a segment. Because on the one hand the mass of solar arrays can magnitude to an amount which can cause instable roll moments so that the HAP could tilt upside down. On the other hand for particular designs the required size of solar arrays could be much greater than the available size of installation surface of the segments. Therefore the maximum portable size of solar arrays of a LTA HAP is restricted.

However, for certain designs with higher mean wind velocities and corresponding larger energy usage requires a huge amount of solar arrays. Thus with aforementioned restrictions the maximum wind velocity is therefore limited for designs for northern latitudes of 48.83° and altitudes of 20km. These values lie between 13-14m/s for state of the art solar arrays and battery storage technology.

The design for winter months requires 5 times more solar array area as the designs of summer months, thus with the state of the art technology such designs are not attainable and therefore a station keeping task in our latitude is not possible.

A comparison with conventional airships reveals that the values of the constraint lines of design surface have almost the same values as that of chainbody LTA HAP. Thus the design space of conventional airships has similar limitations as that of chainbody LTA HAP. However chainbody LTA HAP have much more structural benefits over conventional airship concepts for station keeping tasks in 20 km altitudes.

Further investigation yields that the constraint lines can be shifted by increasing the specific mass and solar array efficiency. With $0.25\text{kg}/\text{m}^2$ and 41% wind velocities up to 28m/s can be obtained. But for these mean wind velocities solar array areas as big as football fields are required. It is doubtful, whether these size of areas can be handled sufficiently on flexible membranes. With a theoretical value of efficiency of more than 75%

and specific mass of about $5g/m^2$ feasible design could be achieved.

Beside the solar array technology it is desirable to utilize a electrical storage technology with higher energy density than the state of the art technology with $156Wh/kg-1,8kWh/kg$ in order to achieve high performance designs. Electrical storage systems with capacities up to $13kWh/kg$ has to be developed; this is a value near to capacity of contemporary fossile fuels.

Outlook:

The developed object oriented graph grammar based design language provides the opportunity of further development of the design model with regard to the level of detail of each discipline according to the state of the art. Moreover further analysis can be integrated to the design model, such as:

- FEA of the membrane of envelope,
- material models
- CFD analysis (computational fluid dynamics)
- flight dynamic model for control design
- detailed model of the battery and fuelcell, etc.

Thus it is possible to enhance the model of each discipline in arbitrary depth and perform a multidisciplinary design analysis.

In regard to the technological aspect there is enough development potential primarily in the field of solar cell research. Only through the use of solar cells with very low specific mass and high efficiencies design of chainbody LTA HAP can be obtained with sufficient mean wind velocities and handleable size of envelope, solar cell area and energy storage system.

Bibliography

- [1] AGARWAL, M.; CAGAN, J. and K. CONSTANTINE: *Influencing generative design through continuous evaluation: associating costs with the coffeemaker shape grammar in AIEDAM*. 1999.
- [2] AGARWAL, M. and J. CAGAN: *Shape Grammars and their languages, A methodology for product design and product representation in ASME*. 1997.
- [3] AGARWAL, M. and J. CAGAN: *A blend of different tastes: the language of coffeemakers in Environmental Planning*. 1998.
- [4] ALBER, R. and S. RUDOLPH: *On a grammar-based design language that supports automated design generation and creativity, Proceedings of IFIP WG5.2 Workshop on Knowledge Intensive CAD (KIC-5), Malta*. 2002.
- [5] ALBER, R. and S. RUDOLPH: *43 - a generic approach for engineering design grammar, Proceedings of American Association for Artificial Intelligence, Spring Symposium Technical Report*. 2003.
- [6] ALBER, R.; RUDOLPH, S. and B. KRÖPLIN: *On formal languages in design generation and evolution, WCCMV, Fifth World Congress on Computational Mechanics, Vienna, Austria*. 2002.
- [7] ANTONSSON, E. and J. CAGAN: *Formal Engineering Design Synthesis, Developments in formal design synthesis methods, Cambridge University Press*. 2005.
- [8] BALDWIN, R. and J. CHUNG, M.: *Design Methodology Management Using Graph Grammars*. 1994.
- [9] BERNASCONI, M.: *Going Elsewhere - Adapting Structures for Use in Space through Rigidizing Materials, Fraunhofer, IRB*. 2006.
- [10] BÖLLING, M.: *Multidisziplinärer Luftschiffentwurf mit einer graphenbasierten Entwurfssprache, DGLR Workshop VIII Luftfahrzeuge leichter als Luft*. 2005.

-
- [11] BOEING: *Spectrolab Inc., Solar cell breaks 40% efficiency barrier*, www.insidegreentech.com/node/454. 2006.
- [12] BURNETT, B.: *The basic physics and design of III-V multijunction solar cells*. 2002.
- [13] CAGAN, JONATHAN; CAMPBELL, M. F.-S. and T. TOMIYAMA: *A Framework for Computational Design Synthesis: Model and Applications*. Journal of Computing and Information Science in Engineering, 2005.
- [14] CATIA: *CATIA V5, Dassault Systems, Internet: www.3ds.com*. 2011.
- [15] CETIN, O., L. and K. SAITOU: *Decomposition-based assembly synthesis of multiple structures for minimum production cost*. 2003.
- [16] CETIN, O., L. and K. SAITOU: *Decomposition-Based Assembly Synthesis for Maximum Structural Strength and Modularity*. Journal of Mechanical Design, 2004.
- [17] CETIN, O. and K. SAITOU: *Decomposition-Based Assembly Synthesis for Structural Modularity*. 2004.
- [18] CETIN, O. L.: *Decomposition based assembly synthesis of family of structures*. 2003.
- [19] CHEN, L. and S. LI: *Analysis of decomposability and complexity for design problems in the context of decomposition*. Journal of Mechanical Design, 2005.
- [20] CHOMSKY, N.: *Three models for the description of models*. MIT, 1949.
- [21] COLOZZA, A.: *Initial Feasibility Assessment of a High Altitude Long Endurance Airship*, 2003.
- [22] COLOZZA, A. and J. DOLZE: *High-Altitude, Long-Endurance Airships for Coastal Surveillance (NASA)*, 2005.
- [23] CYPRESS: *HPL Series Permanent Magnet Motors - Product Brochure, Canopy Technologies, LLC*. 2010.
- [24] DAIMLER, A. G.: *Shaping Future Transportation. Clean Drive Technologies..* 2009.
- [25] DEB, K.: *Multi-Objective Evolutionary Algorithms, Kanpur Genetic Algorithm Laboratory, Indian Institute of Technology Kanpur*. 2005.
- [26] DIMROTH, F.: *3-6 junction photovoltaic cells for space and terrestrial application, Photovoltaic Specialists Conference*. 2005.

- [27] DIN-ISO-2533: *Normatmosphäre*. Berlin: Beuth. 1979.
- [28] DRELA, M.: *XRotor user guide*, MIT. 1996.
- [29] DU, X.; JIAO, J. M.-M. and M. TSENG: *Graph Grammar Based Product Family Modeling*. Concurrent Engineering: Research and Application, 2002.
- [30] DU X., JIAO, J. and M. TSENG: *Modelling platform-based product configuration using programmed attributed graph grammars*. Journal of Engineering Design, 2003.
- [31] FINGER, S. and R. RINDERLE, J.: *A transformational approach to mechanical design using a bond graph grammar*, *Proceedings of the First ASME Design Theory and Methodology Conference*. 1989.
- [32] FRANK, P.: *Die Auslegung von Flugzeugen mit geringstem Antriebsleistungsbedarf*. Dissertation, Institut für Flugzeugbau, Universität Stuttgart. 1992.
- [33] GADIR, Y. A.: *Ballone und Luftschiffe*, 2001.
- [34] GLOBAL-WARMING: *Global Warming Art*, Robert A. Rohde, Internet: www.globalwarmingart.com. 2011.
- [35] GLUNZ, S.: *n-Type Silicon-Enabling efficiencies > 20production*, Fraunhofer ISE Freiburg, 35th PYSC Honolulu, Hawaii. 2010.
- [36] GRACE, D.; THORNTON, J. and T. KONEFAL: *Broadband Communications from High Altitude Platforms - The HeliNet Solution*, 2002.
- [37] GREIF, A.: *Untersuchungen an Geschalteten Reluktanzantrieben für Elektrofahrzeuge*. Dissertation, Institut für Elektrische Antriebstechnik, Universität der Bundeswehr, München- Neubiberg. 2000.
- [38] GÖTTLER, H.: *Graphgrammatiken in der Softwaretechniken*, 1988.
- [39] GUTER, W.: *Current-matched triple-junction solar cell reaching 41.1conversion efficiency under concentrated sunlight*, *Applied Physics*. 2009.
- [40] HALL, D.; FORTENBACH, C. D.-E. and R. PARKS: *A Preliminary Study of Solar Powered Aircraft and Associated Power Trains*. Lockheed Missiles and Space Company. NASA-Contractor Report-3699, Sunnyvale (California). 1983.
- [41] HAMILTON: *Standard, Division of united aircrafts: Generalized Method of Propeller Performance Estimation*. Windsor Locks (Connecticut). 1963.

- [42] HAQ, M. and B. KRÖPLIN: *Topological design of a High Altitude Platform System (HAP) using a system design language in 1st CEAS European Air and Space Conference*. 2007.
- [43] HAQ, M. and S. RUDOLPH: *Design acceleration of automotive structures by structure design language*. 2006.
- [44] HAQ, M. and S. RUDOLPH: *A design language for generic space-frame structure design*. International Journal of Computer Applications in Technology, 2007.
- [45] HEPPELLE, M.: *Ein Computerprogramm für Entwurf und Analyse von Propellern, Diplomarbeit, Institut für Flugzeugbau, Universität Stuttgart*. 1984.
- [46] HI-PA-DRIVE: *PML Flightlink*. <http://www.pmlflightlink.com/motors/hipa-drive.html>. 2010.
- [47] HIMAX: *Brushless Outrunner Motor HC6332-250"*. Maxx Products International, Inc.. 2010.
- [48] HINDLE, S.: *Sky Tower High Altitude Platform Stations (HAPS) for Wireless Broadband and other High Value Applications*, 2001.
- [49] HIRNER, A.: *Entwurf eines Verstellpropellers für die Stratosphärenplattform Luftwurm 2.0*. 2006.
- [50] HÖLTTÄ-OTTO, K.: *Modular Product Platform design*. 2005.
- [51] HOBUS, F.: *Konstruktion und Berechnung eines Verstellpropellers in Faserverbundbauweise für eine Stratosphärenplattform, Universität Stuttgart, Institut für Flugzeugbau*. 2006.
- [52] HOERNER, S.: *Fluid Dynamic Drag*. 1965.
- [53] IILS: *Entwurfscompiler 43TM is Trademarks of IILs mbH, Stuttgart*. 2005.
- [54] IQBAL, M.: *An Introduction to Solar Radiation, Canada: Academic Press*. 1983.
- [55] IRANI, M. and S. RUDOLPH: *Design grammars for conceptual design of space stations, Proceedings of IAC, IAC-03-T.P.02, Bremen, Germany*. 2003.
- [56] ISO-5878: *Reference atmospheres, ADDENDUM 1: Wind supplement*. Berlin. 1983.
- [57] JEWELL, G.: *Permanent Magnet Machines and Actuators. Symposium on Materials for a Sustainable Future. Birmingham, England: Magnetic Materials Group, University of Birmingham*. 2009.

- [58] JONES, S., P.: *Aerodynamic Estimation Techniques for Aerostats and Airships, Journal of Aircraft, Vol. 20, No. 2.* 1983.
- [59] KEIDEL, B.: *Auslegung und Simulation von hochfliegenden dauerhaft stationierbaren Solardrohnen.* 2000.
- [60] KIT: *Einführung in die Ingenieur- und Hydrogeologie, KIT Karlsruhe Institute of Technology.* 2004.
- [61] KORMEIER, T.; ALBER, R. and S. RUDOLPH: *Topological and parametrical design of aircraft surfaces using design grammars, Proceedings of DGLR Symposium German Aerospace Congress, Munich, Germany.* 2003.
- [62] KORMEIER, T.: *Graphenbasierte Entwurfssprachen zur konsistenten Modellierung und musterbasierten Topologiemodifikation von Faserverbundstrukturen.* 2010.
- [63] KORMEIER, T. and S. RUDOLPH: *On Self-Similarity As A Design Paradigm in ASME.* 2005.
- [64] KÜPPER, A. and M. SCHLICHTENMAYER: *Photovoltaik und Brennstoffzelle, Versuch E219, Physikalisches Praktikum für Fortgeschrittene.* 2004.
- [65] KRÖPLIN, B.; EPPERLEIN, F. and A. KUNZE: *Mechanical aspects of flight in the lower stratosphere in Shell Structure: Theory and Applications, Francis Group, London.* 2006.
- [66] KUSIAK, A.: *Engineering Design, products, Processes, and Systems.* 1999.
- [67] LAN, C. and J. ROSKAM: *Airplane Aerodynamics and Performance. Kansas: Roskam Aviation and Engineering Corporation.* 1981.
- [68] LANGE: *EA 42 series engines, EASA Type-certificate data sheet, Lange Flugzeugbau GmbH.* 2006.
- [69] LARRABEE, E.: *Practical design of a minimum loss propeller, SAE Technical Paper.* 1979.
- [70] LÜDECKE, A.: *Simulation gestützte Verfahren für den Top-Down-Entwurf heterogener Systeme, Universität Duisburg-Essen.* 2003.
- [71] LEE, YUNG-GYO, K. D.-M. and C.-H. YEOM: *Development of Korean High Altitude Platform System.* International Journal of Wireless Information Networks, 2005.

- [72] LEWIS, JAMISON, G. S. S. and R. P. I. ISAAC: *High-Altitude Airships for the Future Force Army*, 2005.
- [73] LI, XIN; SCHMIDT, L. H.-W. L. L. and Y. QIAN: *Transformation of an EGT-Grammar: New Grammar, New Design*. *Journal of Mechanical Design*, 2004.
- [74] LI, X. and S. L.: *Grammar-based designer assistance tool for epicyclic gear trains*. *Journal of Mechanical Design*, 2004.
- [75] LI, Y.: *Dynamics Modeling and Simulation of Flexible Airships*. 2008.
- [76] LI, Y. and M. NAHON: *Modelling and Simulation of Airship Dynamics, Journal of Guidance, Control and Dynamics Vol.30, No. 6*. 2007.
- [77] LIPPERT, T.: *Auslegung des Antriebsstranges einer hochfliegenden Solardrohne, FH-München und Institut für Flugmechanik, Deutsche Forschungsanstalt für Luft- und Raumfahrt, Braunschweig*. 1998.
- [78] LOCKHEED, M.: *HALE-D, Lockheed Martin Corporation, Internet: www.lockheemartin.com/ms2*. 2008.
- [79] LT-SPICE: *Linear Technology Corporation, Internet: www.linear.com*. 2010.
- [80] LUFFMAN, C., R.: *Lighter-Than-Air High Altitude Platform Feasibility Study, LTA Solutions*. 2004.
- [81] LYU, N. and K. SAITOU: *Decomposition-Based Assembly Synthesis of a 3D Body-In-White Model for Structural Stiffness*. 2000.
- [82] LYU, N. and K. SAITOU: *Topology Optimization of Multicomponent Beam Structure via Decomposition-Based Assembly Synthesis*. *Journal of Mechanical Design*, 2005.
- [83] MATHEMATICA: *http://www.wolfram.com*. 2003.
- [84] MCCORMACK, J. and J. CAGAN: *Designing inner hood panels through a shape based framework, Artificial Intelligence for Engineering Design, Analysis and manufacturing, Cambridge University Press*. 2002.
- [85] MERZIGER, G. and T. WIRTH: *Repetitorium der Höheren Mathematik, Binomi Verlag*. 2006.
- [86] MÜLLER, B.: *Strom auf Vorrat, Energie*. 2009.
- [87] MULLINS, S. and J. RINDERLE: *Grammatical Approaches to Engineering Design, Part I: An Introduction and Commentary*. *Research in Engineering Design*, 1991.

- [88] NAESUNG, L. and K. SAITOU: *Decomposition-Based Assembly Synthesis Based on Structural Stiffness Consideration in ASME 2002*. 2002.
- [89] NAGL, M.: *Graphenbasierte Werkzeuge zur Unterstützung des Konzeptuellen Gebäude-Etwurfs*, 2005.
- [90] NEIL, D.: *Honda FCX Clarity: Beauty for beauty's sake*, *Los Angeles Times*. 2009.
- [91] NILSSON, ERIK; NORDHAGEN, E. and O. GRO: *Aspects of Systems Integration, Center of Industrial Research, Oslo, Norway*. 1991.
- [92] NOAA: NASA/USAF: *U.S. Standard Atmosphere*. Washington D.C.: U.S. Government Printing Office. 1976.
- [93] OHL, M.: *Elektrolyse und Brennstoffzelle, Institut für Energiewirtschaft und Rationelle Energieanwendung, Universität Stuttgart*. 2005.
- [94] PAHL, G. and W. BEITZ: *Engineering Design A systematic approach*. 2007.
- [95] PALLAVICINI, B.: *Automatic guidance strategies for HALE solar airplanes with pivoting panels. Diplomarbeit, Deutsches Zentrum für Luft- und Raumfahrt, Braunschweig*. 1999.
- [96] PAVLIDOU, F.; MIURA, R. and J. FARSEROTU: *High Altitude Platform (HAP) Systems: Technologies and Applications, Wireless Personal Communications; 32: 189-194; DOI: 10.1007/s11277-005-0741-4 Springer*. 2005.
- [97] PETERMANN, K.; FRIEDRICH, J. and M. OETKEN: *Schwierigkeiten auf dem Weg ins Diskontinuum - Eine an Schülervorstellungen orientierte Unterrichtseinheit zur Einführung des Kugelteilchenmodells*. 2010.
- [98] PRUSINKIEWICZ, P; LINDENMAYER, A.: *The algorithmic beauty of plants*. 1990.
- [99] PUGLIESE, M. and C. JONATHAN: *Capturing a rebel: modeling the Harley-Davidson brand through a motorcycle shape grammar*. *Research in Engineering Design*, 2002.
- [100] REED, K.: *Market Potential of CP1/a-Si:H Thin Film Solar Cells for Space and HAA Applications, SESCRC*. 2006.
- [101] REED, K.: *Gigawatt Space and Terrestrial manufacturing, two sides of the same solar energy coin, ISDC Washington DC*. 2008.
- [102] REHMET, M.: *Eine Methode zur Auslegung von Solarflugzeugen. Dissertation, Institut für Statik und Dynamik der Luft- und Raumfahrtkonstruktionen, Universität Stuttgart*. 1997.

- [103] REHMET, M. and B. KRÖPLIN: *Beschreibung der Ausrüstung und des Antriebssystems des Solarflugzeuges icaré 2. ISDBericht Nr. 96/2, Institut für Statik und Dynamik der Luft- und Raumfahrtkonstruktionen, Universität Stuttgart.* 1996.
- [104] RIMFIRE: *Great Planes ElectriFly RimFire 65cc 80-85-160 Brushless Outrunner Electric Motor.* 2010.
- [105] SCHAEFER, J. and S. RUDOLPH: *Satellite design by design grammars, Aerospace Science and Technology, Vol. 9, pp.81-91.* 2005.
- [106] SCHÄFER, I.: *HALE aerostatic platforms, applications, maturity and research demands, USE-HAAS Workshop, Brussels.* 2005.
- [107] SCHMIDT, L.; SHI, H. and S. KERKAR: *A constraint satisfaction problem approach linking function and grammar-based design generation to assembly.* Journal of Mechanical Design, 2005.
- [108] SCHMIDT, LINDA; SHETTY, H. and C. CHASE, SCOTT: *A Graph Grammar Approach for Structure Synthesis of Mechanisms.* Journal of Mechanical Design, 2000.
- [109] SCHMIDT, D., K.: *Dynamic Modeling, Control and Station-Keeping Guidance of a Large High-Altitude (Near-Space) Airship, AIAA.* 2006.
- [110] SCHMIDT, L. and J. CAGAN: *Grammars for Machine Design in Artificial Intelligence in Design '96.* 1996.
- [111] SCHMIDT, L. and J. CAGAN: *A Graph Grammar-Based Machine Design Algorithm.* Research in Engineering Design, 1997.
- [112] SCHRÖDER, C.: *Toyota optimiert Brennstoffzellen-Fahrzeug: 850 Kilometer ab -30°C, ATZ online.* 2008.
- [113] SCHULZE, J.: *Stromversorgung, Strom auf Vorrat speichern, Konstruktionspraxis.de.* 2010.
- [114] SERVICE, T.-S. I.: *List of fuel-cell vehicles: <http://h2mobility.org/>.* 2010.
- [115] SHEA, K.: *Essays of Discrete Structures: Purposeful Design of Grammatical Structures by Directed Stochastic Search.* 1997.
- [116] SHEA, K. and J. CAGAN: *Innovative dome design: applying geodesic patterns with shape annealing, AIEDAM.* 1997.
- [117] SMOLINKA, T.: *Elektrolyse-produzieren Sie Ihren Wasserstoff selbst, Fraunhofer-Institut für Solare Energiesysteme ISE.* 2007.

- [118] SMOLINKA, T. and M. VETTER: *Vanadium-Redox-Flow-Batterien, Fraunhofer-Institut für Solare Energiesysteme ISE*. 2010.
- [119] SRINDHARAN, P. and M. CAMPBELL: *A Grammar for function structures in ASME*. 2004.
- [120] STINY, G.: *Ice-ray: a note on the generation of Chinese lattice designs in Environmental Planning*. 1977.
- [121] STINY, G.: *Introduction to shape and shape grammars in Environmental Planning*. 1980.
- [122] STINY, G.: *The algebras of design in Research in Engineering Design*. 1991.
- [123] STINY, G. and J. GIPS: *Shape grammars and the generative specification of painting and sculpture in Freiman CV (ed) Information Processing 71. North Holland, Amsterdam*. 1972.
- [124] STINY, G. and J. GIPS: *Production systems and grammars: a uniform characterization in Environmental Planning*. 1980.
- [125] STINY, G. and W. MITCHELL: *The Palladian grammar in Environmental Planning*. 1978.
- [126] STINY, G. and W. MITCHELL: *The grammar of paradise: on the generation of Mughul gardens in Environmental Planning*. 1980.
- [127] STONE, R. B. and K. WOOD: *Development of a functional basis for design*. Journal of Mechanical Design, 2000.
- [128] TOZER, T. C. and D. GRACE: *HeliNet The European Solar-Powered HAP Project*, 2002.
- [129] WEBER, E.: *HYSOLAR: German-Saudi Joint Program on Solar Hydrogen Production and Utilization. Phase II, 1992-1995. Deutsche Forschungsanstalt für Luft- und Raumfahrt e.V. (DLR), Stuttgart; King Abdulaziz City for Science and Technology (KACST), Riyadh*. 1996.
- [130] WEBER, E.: *Semiconductor Defect Science and Technology Opening the Door for the Future of Solar Energy, Fraunhofer ISE*. 2009.
- [131] WESTFECHTEL, B.: *Ein graphbasiertes Managementsystem für dynamische Entwicklungsprozesse. Informatik 16, 125-144*. 2001.
- [132] WILL, J.: *Beitrag zur Standsicherheitsberechnung im geklüfteten Fels in der Kontinuums- und Diskontinuumsmechanik unter Verwendung impliziter und expliziter Berechnungsstrategien*. 1999.

-
- [133] WYOMING: *University of Wyoming, College of Engineering, Department of Atmospheric Science, 10739 Weather Station Stuttgart Schnarrenberg*. 2011.
- [134] YASTREBOVA, N.: *High-Efficiency multi junction solar cells: Current status and future potential, Centre for Research in Photonics, University of Ottawa*. 2007.
- [135] YETIS, F., A. and K. SAITOU: *Decomposition-Based Assembly Synthesis Based on Structural Consideration*. *Journal of Mechanical Design*, 2002.
- [136] YOUNG, A.; ARDEMA, D. and N. MAYER: *Mission And Vehicle Concepts For Modern Propelled Lighter-Than-Air Vehicles*. *Agard-R-724*. 1985.
- [137] YUSAN, H. and S. RUDOLPH: *A study of constraint management integration into the conceptual design phase in ASME Design Engineering Technical Conference*. 1999.
- [138] ZAHORANSKY, R.; ALLELEIN, H. and U. SCHELLING: *Energietechnik, Systeme zur Energieumwandlung, Kompaktwissen für Studium und Beruf, Vieweg-Teubner*. 2010.
- [139] ZAVALA, ARAGON; RUIZ, C. and D. PENIN: *High-Altitude Platforms for Wireless Communication*, 2008.
- [140] ZINNIKER, R.: *Merkblatt Batterien und Akkus, ETH Institut für Elektronik, Zürich*. 2003.